JOURNAL OF SPACECRAFT AND ROCKETS
Vol. 47, No. 4, July–August 2010

Dynamics of Gas Evacuation from a Honeycomb Structure Having Common Wall Perforations

Chun P. Lee
Combustion Research and Flow Technology, Inc., Huntsville, Alabama 35801
Amrutur V. Anilkumar*
Vanderbilt University, Nashville, Tennessee 37235
and
Richard N. Grugel†
NASA Marshall Space Flight Center, Huntsville, Alabama 35812

DOI: 10.2514/1.41883

A model has been developed to provide insight regarding the time to evacuate gas from a sealed structure consisting of elongated hexagonal cells for which the common walls share a relatively small pinhole. Gas flow from a single cell to a vacuum environment, and then between two connected cells, is first considered. The analysis is then applied to a linear string of attached cells, where the pressure drop from the center cell through the edge cell as a function of time and number of intermediate cells is evaluated. Both adiabatic and isothermal conditions were investigated, with the latter resulting in faster drain times. A scaling relationship of the pressure drop between time and the number of cells was found and used to extend the model to the more complicated, two-dimensional hexagonal array problem. Considering an array based on a typical common bulkhead geometry, and applying the isothermal condition, a best-case evacuation time for argon was predicted.

I. Introduction

NASA'S next-generation space transport vehicle, Ares I, is being built to replace the shuttle and eventually return humans to the moon. The second stage houses the liquid oxygen (LOX) and liquid hydrogen (LH2) tanks that will fuel the vehicle's J2-X engine after jettisoning off the solid rocket boosters. Here, the tanks, based in part on the Saturn rocket design, will share what is termed a common bulkhead. Briefly, this is a volume constrained by, generally, the dome-shaped top of the lower (aft) oxygen tank that is separated by 5–10 cm from the bottom of a similarly contoured upper (forward) hydrogen tank. Primary advantages of a common bulkhead include decreasing both the rocket's length and weight; disadvantages include increased design, fabrication, and testing challenges. Separation of the tanks is necessary to keep the lower-temperature LH2 (∼15 K) isolated from the warmer LOX (∼56 K). With that in mind, structural continuity within the common bulkhead is traditionally sustained by adhesively bonding a phenolic honeycomb structure, such as shown in Fig. 1, to the respective top and bottom tank surfaces.

The honeycomb should have poor heat conductivity properties and must be permeable to gas flow in order to fill the structure with, for example, argon for storage and helium for leak checks. Conversely, this same gas needs to be pumped out to minimize conduction (helium gas is highly conductive and will not solidify), eliminate honeycomb degradation from pressure changes or freeze/thaw cycles, and even to reduce weight. Thus, it is necessary that the cell walls have some degree of perforation to ensure gas flow through the honeycomb structure. The size and number of perforations in a cell for each honeycomb application cannot be verified, but it seems reasonable to assume they are on the order of 0.5 mm and number four to eight per cell. These numbers, particularly in combination with the adhesive bonding to the metal dome surfaces, do not compromise the structural integrity of the honeycomb.

The following idealized scenario illustrates the magnitude of a presumed honeycomb geometry corresponding to a reasonably sized common bulkhead. First, consider a 635 cm (250 in.)-diameter sphere. A dome section having a bottom diameter of 548.64 cm (216 in.) is cut from this sphere and represents the outer limit of the common bulkhead. The periphery of this dome section is open, and the honeycomb is assumed to cover the top of the dome to a diameter of 538.48 cm (212 in.). The honeycomb consists of small thin-walled hexagonal cells having a distance of ∼0.46 cm (0.1811 in.) between opposing walls and an assumed height of 6.096 cm (2.4 in.). Another dome (bottom of the LH2 tank), of an obviously different diameter, sits above the lower one (top of LOX tank), such that the cell height is maintained.

A single hexagonal cell is assumed at the apex of the lower dome, and the arc length from this cell's center to the outer diameter limit (538.48 cm) of the honeycomb core is 321.31 cm (126.5 in.). Recalling the base cell length of ∼0.46 cm, an arc segment can then be envisioned as a row of 699 individual cells; note here that gas in the apex cell must pass through at least 698 cells to be removed from the honeycomb. Maintaining the hexagonal grid pattern, the apex cell is surrounded by an initial ring of six abutting cells. The second ring consists of 12 cells, and each sequential ring is increased by six cells over the previous. The total number of cells comprising this common bulkhead, from the apex through the 698th ring, consequently numbers 1,463,707. The volume of an individual cell is ∼1.117 cm^3, which sums to approximately 1635 liters (432 gal). Again, note that the density of argon at standard temperature and pressure is ∼0.0017859 kg/l, which given the honeycomb volume, corresponds to some 2.92 kg (6.424 lb) of unnecessary weight.

The above introduction gave a general understanding of the geometry, magnitude, and role the honeycomb plays in the common bulkhead. Reasons for filling it with gas, as well removing gas, were mentioned; a long and perceivably difficult/time-consuming gas-evacuation path was implied. Monitoring the pressure drop during evacuation would be straightforward if gauges could be inserted along the length through the dome caps into the honeycomb; this, unfortunately, is clearly impossible from a design perspective.

Received 29 October 2008; revision received 14 April 2010; accepted for publication 16 April 2010.

*Department of Mechanical Engineering.
†EM-30.

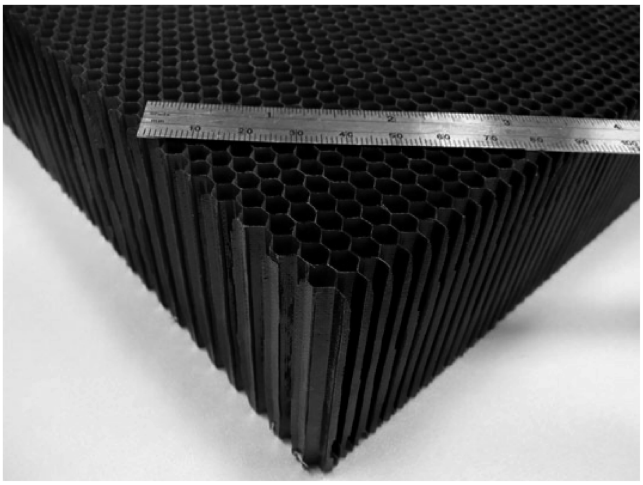

Fig. 1 Photograph of a phenolic honeycomb structure, which typifies that considered in the analysis.

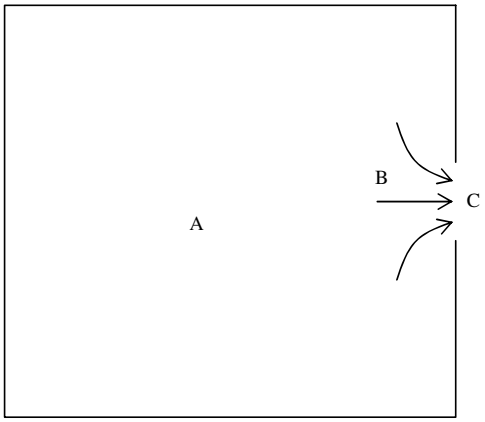

Fig. 3 *A* is a point inside the cavity far from the hole, for which the dimension is much smaller than those of the cavity. At *A*, the fluid can be considered as quiescent. *B* is a point near the hole, where the fluid suddenly picks up a large velocity upon being forced out of the cavity, Around *B*, well-defined streamlines appear. *C* is a point at the hole, where the velocity is equal to the local speed of sound in a choked flow.

The intent of the following is to present a dynamic model that predicts changes in gas pressure as a function of distance from the central cell over time. Such information is necessary to determine the time to reach the desired core vacuum level. Consequences of a partial evacuation include obtaining inaccurate test results, possibly poor performance and/or shortened lifetime, and potential failure.

II. Definition of the Problem

Consider a structure in a vacuum consisting of a series of finite numbers of closed cells of arbitrary shapes and sizes, separated by thin walls. Let the cells be filled with a gas at p_0 and T_0. Consider the structure being punctured, for example, by a laser beam, such that a series of cells are linked by holes along the beam path from one side to the other (Fig. 2). Let the punctured cells be labeled by i, from 1 to N, going from the entry to the exit of the beam. The question is how the gas in the cells defined by the beam path drain to adjacent cells and the environment.

III. Theoretical Model for a Single Cell

A. Choked Flows

Consider a closed cell of volume V with a thin wall that contains a gas at pressure p and temperature T. If the outside environment is a vacuum, and a small hole is suddenly punched through the cell wall, the gas will rush out as a choked flow (under the title critical velocity in Landau and Lifshitz [1]), as illustrated in Fig. 3.

Referring to Fig. 3, there is no flow at point A. The gas in the cell is considered to be uniform at large, except for the negligible volume of flow near the hole. According to conservation of mass, in case of leakage,

$$V\frac{\mathrm{d}\rho}{\mathrm{d}t} = -\rho' u' a \tag{1}$$

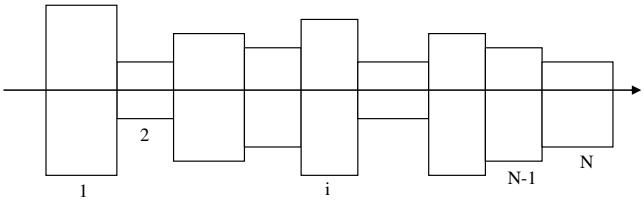

Fig. 2 Ideally, the *n* punctured cavities can be lined up along the beam and labeled accordingly from 1 to *n*.

where t is time, V is the volume of the cell, ρ is the uniform density of the gas in the cell, ρ' and u' are the density and velocity of the gas at the hole, and a is the area of the hole. The path from the quiescent point A to the hole C consists of two parts: from A to B and from B to C.

The transition from A to B along a streamline can be considered as adiabatic, since a slowly drifting fluid element experiences a significant pull toward the hole only when it is near the hole. The temperature T_B, speed of sound c_B, density ρ_B, and pressure p_B at B are given by

$$\frac{T}{T_B} = 1 + \frac{\gamma - 1}{2}M^2 \tag{2}$$

$$\frac{c^2}{c_B^2} = 1 + \frac{\gamma - 1}{2}M^2 \tag{3}$$

$$\frac{\rho}{\rho_B} = \left(1 + \frac{\gamma - 1}{2}M^2\right)^{\frac{1}{\gamma - 1}} \tag{4}$$

$$\frac{p}{p_B} = \left(1 + \frac{\gamma - 1}{2}M^2\right)^{\frac{\gamma}{\gamma - 1}} \tag{5}$$

where γ is the ratio of specific heats, $c = (\gamma RT)^{1/2}$ is the sound speed in the cell (with R being the gas constant per unit mass), and $M = u_B/c$.

The transition from B to C along a streamline, in the case of the establishment of a choked flow, can be considered as even more adiabatic, since the velocity u' is in the process of attaining the local speed of sound c^*. The quantities at C, marked by an asterisk (*), are related to the quiescent quantities at A in the cell, through the dynamic quantities at B, by using Eqs. (2–5) as

$$\frac{c^{*2}}{c^2} = \frac{2}{\gamma + 1} \tag{6}$$

$$\frac{T^*}{T} = \frac{2}{\gamma + 1} \tag{7}$$

$$\frac{p^*}{p} = \left(\frac{2}{\gamma+1}\right)^{\gamma/(\gamma-1)} \tag{8}$$

$$\frac{\rho^*}{\rho} = \left(\frac{2}{\gamma+1}\right)^{\gamma/(\gamma-1)} \tag{9}$$

The mass flow rate through the hole at C is given by $\rho' u' a = \rho^* c^* a$, such that by using Eqs. (6) and (9), Eq. (1) becomes

$$\frac{\mathrm{d}\rho}{\mathrm{d}t} = -\frac{a}{V}\left(\frac{2}{\gamma+1}\right)^{(\gamma+1)/[2(\gamma-1)]} (\gamma p \rho)^{1/2} \tag{10}$$

Beginning with Eq. (10), we have to consider the walls as being either adiabatic or isothermal.

If the wall is adiabatic, then using $\rho = \rho_0 (p/p_0)^{1/\gamma}$, where ρ_0 and p_0 are the initial values of ρ and p in the cell, respectively, we have

$$\frac{\mathrm{d}p}{\mathrm{d}t} = -\gamma\left(\frac{2}{\gamma+1}\right)^{(\gamma+1)/[2(\gamma-1)]} \frac{a}{V} c_0 p_0 \left(\frac{p}{p_0}\right)^{(3\gamma-1)/2\gamma} \tag{11}$$

Here, $c_0 = (\gamma R T_0)^{1/2}$ is the speed of sound in the cell at the initial temperature T_0, and p_0 is the initial pressure. The solution of this equation is

$$\frac{p}{p_0} = \frac{1}{[1 + (\frac{\gamma-1}{2})(\frac{2}{\gamma+1})^{(\gamma+1)/[2(\gamma-1)]} \frac{a}{V} c_0 t]^{2\gamma/(\gamma-1)}} \tag{11a}$$

If the wall is isothermal (i.e., T is constant at T_0), then by using $\rho = p/RT_0$, the rate of loss of pressure in the gas from Eq. (10) is

$$\frac{\mathrm{d}p}{\mathrm{d}t} = -\left(\frac{2}{\gamma+1}\right)^{(\gamma+1)/[2(\gamma-1)]} \frac{a}{V} c_0 p \tag{12}$$

The solution of this equation is

$$\frac{p}{p_0} = \exp\left[-\left(\frac{2}{\gamma+1}\right)^{(\gamma+1)/[2(\gamma-1)]} \frac{a}{V} c_0 t\right] \tag{12a}$$

What if the environment is not a vacuum? The choked flow upstream of the hole is independent on what is downstream, and the equations for the choked flow still hold, provided that the pressure p' at C obeys the condition,

$$\frac{p'}{p} \le \left(\frac{2}{\gamma+1}\right)^{\gamma/(\gamma-1)} \equiv \beta \tag{13}$$

Otherwise, leaking takes place at a rate driven by the pressure difference between the two sides of the hole, which is dealt with next.

B. Subcritical Flow

The word subcritical is used for the case of $p'/p > \beta$, in Eq. (13), in the context of choked flow being critical. In this case, the flow depends on the pressures on both the upstream and downstream sides of the hole.

Referring to Fig. 4, let the pressures at A, B, and C be p, p', and p''. Their relation, to be corrected later, is approximated as

$$p' = \tfrac{1}{2}(p + p'') \tag{14}$$

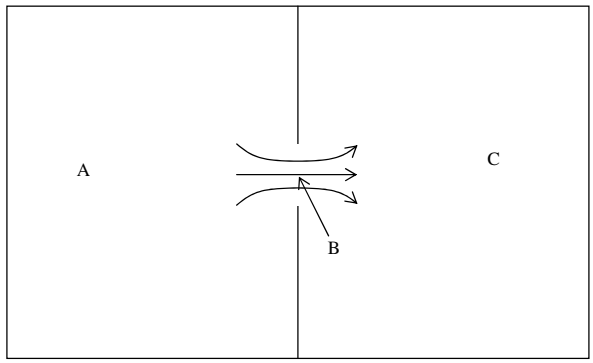

Fig. 4 Two cavities connected by a small common hole. *A* and *C* are quiescent points far from the hole. *B* is a point at the hole. There are well-defined streamlines around the hole.

The Bernoulli equation from A to B is

$$p = p' + \tfrac{1}{2}\rho' u'^2 \tag{15}$$

where the prime refers to quantities at B, where the hole is located. Assuming the transition from A to B as being adiabatic, $\rho' = \rho(p'/p)^{1/\gamma}$. Then, also using u' from Eq. (15), Eq. (1) becomes

$$\frac{\mathrm{d}\rho}{\mathrm{d}t} = -\frac{a}{V}\rho^{1/2}[2(p-p')]^{1/2}\left(\frac{p'}{p}\right)^{1/2\gamma} \tag{16}$$

Again, beginning with Eq. (16), we have to consider the walls as being either adiabatic or isothermal.

If the wall is adiabatic, then we have $\rho = \rho_0 (p/p_0)^{1/\gamma}$. Substituting this into Eq. (16) and using $2(p-p') = p - p''$ according to Eq. (14), Eq. (16) becomes

$$\frac{\mathrm{d}p}{\mathrm{d}t} = -C\frac{a}{V}\frac{\gamma p_0^{1/2\gamma}}{\rho_0^{1/2}} p^{1-\frac{1}{\gamma}} p'^{1/2\gamma} (p - p'')^{1/2} \tag{17}$$

If the wall is isothermal, such that T is constant at T_0, we have (in the cell) $\rho = p/RT_0$. Then, Eq. (16) becomes

$$\frac{\mathrm{d}p}{\mathrm{d}t} = -C\frac{a}{V}\frac{c_0}{\gamma^{1/2}} p^{(1/2)[1-(1/\gamma)]} p'^{1/2\gamma} (p - p'')^{1/2} \tag{18}$$

In Eqs. (17) and (18), the pressure p'' of the cell on the downstream side of the hole can be constant for an external reservoir or a similarly time-dependent quantity like p of the adjacent cell. The constant C is a correction factor determined next.

Since Eq. (14) is essentially a guess, it is necessary to check for the consistency of Eqs. (17) and (18) with Eqs. (11) and (12), respectively, when $p'/p = \beta$ in Eq. (13). For $C = 1$, by setting Eqs. (17) and (18) at this limit, it is found that the ratio of the right side of Eq. (11) to that of Eq. (17), as well as the ratio of the right side of Eq. (12) to that of Eq. (18), are both

$$C = \frac{\gamma^{1/2}}{\beta^{1/2\gamma}[2(1-\beta)]^{1/2}}\left(\frac{2}{\gamma+1}\right)^{(\gamma+1)/[2(\gamma-1)]} \tag{19}$$

For monatomic gases such as argon, $\gamma \approx 5/3$ and, consequently, $C = 0.8854$. As this is close to one, the approximation for the subcritical flow is quite good, and $C = 0.8854$ is used as the correction factor.

In applying the Bernoulli principle, Eq. (15), for $p'/p > \beta$, the flow is assumed to be inviscid and stops when $p'/p = 1$. For p'/p approaching one, viscosity becomes important, and Stokes flow is present. However, then the velocity at the hole should be negligible when compared with the speed of sound, and its contribution to the leak can be ignored.

IV. Theoretical Model for a String of *N* Cells

Each cell along the path made by the beam has sinks and sources of gas: the sinks from leaking to vacuum or adjacent cells and the sources from receiving leaking from adjacent cells. Assuming that the holes are much smaller than the dimensions of the cells, the gas in each cell is approximated as quiescent and uniform. Then the results from the last section are applicable.

A. Adiabatic Case

For the $i = 1$ cell in Fig. 5, the pressure is dictated by the leak to the vacuum through the hole on the left, and the exchange of gas with the next cell $i = 2$ through their common hole on the right. To account for the latter, Eqs. (11) and (17) are combined with some additional terms:

$$\begin{aligned}\frac{\mathrm{d}p_1}{\mathrm{d}t} &= -\Gamma_A \frac{a_{1,v}}{V_1} K_A p_1^{\lambda} - \Gamma_A \frac{a_{1,2}}{V_1} K_A p_1^{\lambda} H\left(\beta - \frac{p_2}{p_1}\right) \\ &+ \Gamma_A \frac{a_{1,2}}{V_1} K_A p_2^{\lambda} H\left(\beta - \frac{p_1}{p_2}\right) \\ &- CH_A \frac{a_{1,2}}{V_1} p_1^{1-\frac{1}{\gamma}} \left(\frac{p_1 + p_2}{2}\right)^{\frac{1}{2\gamma}} (p_1 - p_2)^{1/2} H\left(\frac{p_2}{p_1} - \beta\right) \\ &\times H\left(\frac{p_1}{p_2} - 1\right) + CH_A \frac{a_{1,2}}{V_1} p_2^{1-\frac{1}{\gamma}} \left(\frac{p_1 + p_2}{2}\right)^{1/2\gamma} \\ &\times (p_2 - p_1)^{1/2} H\left(\frac{p_1}{p_2} - \beta\right) H\left(\frac{p_2}{p_1} - 1\right) \end{aligned} \tag{20}$$

where p_1 and p_2 are the pressures in cells 1 and 2, respectively, $a_{1,v}$ is the area of the hole of cell 1 leading to vacuum, $a_{1,2} = a_{2,1}$ is the area of the hole between cells 1 and 2, V_1 and V_2 are the volumes of cells 1 and 2, respectively,

$$\Gamma_A = \gamma \left(\frac{2}{\gamma + 1}\right)^{(\gamma+1)/[2(\gamma-1)]} \tag{20a}$$

$$K_A = \frac{c_0}{p_0^{\lambda - 1}} \tag{20b}$$

$$\lambda = \frac{3\gamma - 1}{2\gamma} \tag{20c}$$

$$H_A = \frac{\gamma p_0^{1/2\gamma}}{\rho_0^{1/2}} \tag{20d}$$

and $H(x)$ is the step function defined by $H(x) = 0$ if $x < 0$ and $H(x) = 1$ if $x \geq 1$. In Eq. (20), on the right side, the first term represents the leak to the vacuum, the second term represents the leak from cell 1 to cell 2 by choked flow if $p_2/p_1 < \beta$, the third term represents the leak from cell 2 to cell 1 by choked flow if $p_1/p_2 < \beta$, the fourth term represents the leak from cell 1 to cell 2 by subcritical flow if $p_2/p_1 > \beta$ and $p_1 > p_2$, and the fifth term represents the leak from cell 2 to cell 1 by subcritical flow if $p_1/p_2 > \beta$ and $p_2 > p_1$. Thus, both the critical and subcritical regimes are covered. The third and fifth terms are possible sources for cell 1.

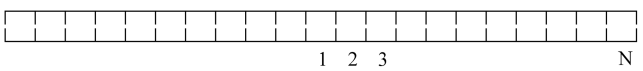

Fig. 5 A string of identical cells for which the common walls share a small perforation.

Similarly, for cells i from two to $N - 1$, the equation is

$$\begin{aligned}\frac{\mathrm{d}p_i}{\mathrm{d}t} &= -\Gamma_A \frac{a_{i-1,i}}{V_i} K_A p_i^{\lambda} H\left(\beta - \frac{p_{i-1}}{p_i}\right) \\ &- \Gamma_A \frac{a_{i,i+1}}{V_i} K_A p_i^{\lambda} H\left(\beta - \frac{p_{i+1}}{p_i}\right) \\ &+ \Gamma_A \frac{a_{i-1,i}}{V_i} K_A p_{i-1}^{\lambda} H\left(\beta - \frac{p_i}{p_{i-1}}\right) \\ &+ \Gamma_A \frac{a_{i,i+1}}{V_i} K_A p_{i+1}^{\lambda} H\left(\beta - \frac{p_i}{p_{i+1}}\right) \\ &- CH_A \frac{a_{i,i-1}}{V_i} p_i^{1-\frac{1}{\gamma}} \left(\frac{p_i + p_{i-1}}{2}\right)^{1/2\gamma} (p_i - p_{i-1})^{1/2} \\ &\times H\left(\frac{p_{i-1}}{p_i} - \beta\right) H\left(\frac{p_i}{p_{i-1}} - 1\right) - CH_A \frac{a_{i,i+1}}{V_i} p_i^{1-\frac{1}{\gamma}} \left(\frac{p_i + p_{i+1}}{2}\right)^{1/2\gamma} \\ &\times (p_i - p_{i+1})^{1/2} H\left(\frac{p_{i+1}}{p_i} - \beta\right) H\left(\frac{p_i}{p_{i+1}} - 1\right) \\ &+ CH_A \frac{a_{i,i-1}}{V_i} p_{i-1}^{1-\frac{1}{\gamma}} \left(\frac{p_i + p_{i-1}}{2}\right)^{1/2\gamma} (p_{i-1} - p_i)^{1/2} \\ &H\left(\frac{p_i}{p_{i-1}} - \beta\right) H\left(\frac{p_{i-1}}{p_i} - 1\right) + CH_A \frac{a_{i,i+1}}{V_i} p_{i+1}^{1-\frac{1}{\gamma}} \left(\frac{p_i + p_{i+1}}{2}\right)^{1/2\gamma} \\ &\times (p_{i+1} - p_i)^{1/2} H\left(\frac{p_i}{p_{i+1}} - \beta\right) H\left(\frac{p_{i+1}}{p_i} - 1\right) \end{aligned} \tag{21}$$

where p_i and V_i are the pressure and volume of cell i, and $a_{i,i+1} = a_{i+1,i}$ is the area of the hole between the adjacent cells i and $i + 1$. On the right side of Eq. (21), the first two terms represent the leak by choked flow of cell i to the adjacent cells $i - 1$ and $i + 1$ if $p_{i-1}/p_i < \beta$ and $p_{i+1}/p_i < \beta$, respectively, and the next two terms represents the gain in cell i due to leaks by choked flow from cells $i - 1$ and $i + 1$ if $p_i/p_{i-1} < \beta$ and $p_i/p_{i+1} < \beta$, respectively. Similarly, the next four terms represent the leak from the cell i to the adjacent cells and the gain of the cell i from the adjacent cells, respectively, by subcritical flow.

For the last cell N, the equation is similar to Eq. (20):

$$\begin{aligned}\frac{\mathrm{d}p_N}{\mathrm{d}t} &= -\Gamma_A \frac{a_{N,v}}{V_N} K_A p_N^{\lambda} - \Gamma_A \frac{a_{N,N-1}}{V_N} K_A p_N^{\lambda} H\left(\beta - \frac{p_{N-1}}{p_N}\right) \\ &+ \Gamma_A \frac{a_{N,N-1}}{V_N} K_A p_{N-1}^{\lambda} H\left(\beta - \frac{p_N}{p_{N-1}}\right) \\ &- CH_A \frac{a_{N,N-1}}{V_N} p_N^{1-\frac{1}{\gamma}} \left(\frac{p_{N-1} + p_N}{2}\right)^{1/2\gamma} \\ &\times (p_N - p_{N-1})^{1/2} H\left(\frac{p_{N-1}}{p_N} - \beta\right) H\left(\frac{p_N}{p_{N-1}} - 1\right) \\ &+ CH_A \frac{a_{N,N-1}}{V_N} p_{N-1}^{1-\frac{1}{\gamma}} \left(\frac{p_{N-1} + p_N}{2}\right)^{1/2\gamma} \\ &\times (p_{N-1} - p_N)^{1/2} H\left(\frac{p_N}{p_{N-1}} - \beta\right) H\left(\frac{p_{N-1}}{p_N} - 1\right) \end{aligned} \tag{22}$$

B. Isothermal Case

For cell 1 in Fig. 5, combining Eqs. (12) and (18), and including appropriate source and sink terms, we have

$$\frac{\mathrm{d}p_1}{\mathrm{d}t} = -\Gamma_I \frac{a_{1,v}}{V_1} c_0 p_1 - \Gamma_I \frac{a_{1,2}}{V_1} c_0 p_1 H\left(\beta - \frac{p_2}{p_1}\right) + \Gamma_I \frac{a_{1,2}}{V_1} c_0 p_2 H\left(\beta - \frac{p_1}{p_2}\right) - C \frac{a_{1,2}}{V_1} \frac{c_0}{\gamma^{1/2}} p_1^{\frac{1}{2}(1-\frac{1}{\gamma})} \left(\frac{p_1+p_2}{2}\right)^{1/2\gamma} (p_1-p_2)^{1/2} \times H\left(\frac{p_2}{p_1}-\beta\right) H\left(\frac{p_1}{p_2}-1\right) + C \frac{a_{1,2}}{V_1} \frac{c_0}{\gamma^{1/2}} p_2^{\frac{1}{2}(1-\frac{1}{\gamma})} \left(\frac{p_1+p_2}{2}\right)^{1/2\gamma} \times (p_2-p_1)^{1/2} H\left(\frac{p_1}{p_2}-\beta\right) H\left(\frac{p_2}{p_1}-1\right) \tag{23}$$

where

$$\Gamma_I = \left(\frac{2}{\gamma+1}\right)^{(\gamma+1)/[2(\gamma-1)]} \tag{23a}$$

For the cells i, from two to $N-1$, following Eq. (23), the equations are

$$\begin{aligned}\frac{\mathrm{d}p_i}{\mathrm{d}t} =& -\Gamma_I \frac{a_{i-1,i}}{V_i} c_0 p_i H\left(\beta - \frac{p_{i-1}}{p_i}\right) - \Gamma_I \frac{a_{i,i+1}}{V_i} c_0 p_i H\left(\beta - \frac{p_{i+1}}{p_i}\right) \\ &+ \Gamma_I \frac{a_{i-1,i}}{V_i} c_0 p_{i-1} H\left(\beta - \frac{p_i}{p_{i-1}}\right) \\ &+ \Gamma_I \frac{a_{i,i+1}}{V_i} c_0 p_{i+1} H\left(\beta - \frac{p_i}{p_{i+1}}\right) \\ &- C \frac{a_{i-1,i}}{V_i} \frac{c_0}{\gamma^{1/2}} p_i^{\frac{1}{2}(1-\frac{1}{\gamma})} \left(\frac{p_{i-1}+p_i}{2}\right)^{1/2\gamma} (p_i - p_{i-1})^{1/2} \\ &\times H\left(\frac{p_{i-1}}{p_i}-\beta\right) H\left(\frac{p_i}{p_{i-1}}-1\right) - C \frac{a_{i,i+1}}{V_i} \frac{c_0}{\gamma^{1/2}} p_i^{\frac{1}{2}(1-\frac{1}{\gamma})} \left(\frac{p_i+p_{i+1}}{2}\right)^{1/2\gamma} \\ &\times (p_i - p_{i+1})^{1/2} H\left(\frac{p_{i+1}}{p_i}-\beta\right) H\left(\frac{p_i}{p_{i+1}}-1\right) \\ &+ C \frac{a_{i-1,i}}{V_i} \frac{c_0}{\gamma^{1/2}} p_{i-1}^{\frac{1}{2}(1-\frac{1}{\gamma})} \left(\frac{p_{i-1}+p_i}{2}\right)^{1/2\gamma} (p_{i-1} - p_i)^{1/2} \\ &\times H\left(\frac{p_i}{p_{i-1}}-\beta\right) H\left(\frac{p_{i-1}}{p_i}-1\right) + C \frac{a_{i,i+1}}{V_i} \frac{c_0}{\gamma^{1/2}} p_{i+1}^{\frac{1}{2}(1-\frac{1}{\gamma})} \left(\frac{p_i+p_{i+1}}{2}\right)^{1/2\gamma} \\ &\times (p_{i+1} - p_i)^{1/2} H\left(\frac{p_i}{p_{i+1}}-\beta\right) H\left(\frac{p_{i+1}}{p_i}-1\right)\end{aligned} \tag{24}$$

For the last cell N, the equation is similar to Eq. (23):

$$\begin{aligned}\frac{\mathrm{d}p_N}{\mathrm{d}t} =& -\Gamma_I \frac{a_{N,v}}{V_N} c_0 p_N - \Gamma_I \frac{a_{N,N-1}}{V_N} c_0 p_N H\left(\beta - \frac{p_{N-1}}{p_N}\right) \\ &+ \Gamma_I \frac{a_{N,N-1}}{V_N} c_0 p_{N-1} H\left(\beta - \frac{p_N}{p_{N-1}}\right) \\ &- C \frac{a_{N-1,N}}{V_N} \frac{c_0}{\gamma^{1/2}} p_N^{\frac{1}{2}(1-\frac{1}{\gamma})} \left(\frac{p_{N-1}+p_N}{2}\right)^{1/2\gamma} \\ &\times (p_N - p_{N-1})^{1/2} H\left(\frac{p_{N-1}}{p_N}-\beta\right) H\left(\frac{p_N}{p_{N-1}}-1\right) \\ &+ C \frac{a_{N-1,N}}{V_N} \frac{c_0}{\gamma^{1/2}} p_{N-1}^{\frac{1}{2}(1-\frac{1}{\gamma})} \left(\frac{p_{N-1}+p_N}{2}\right)^{1/2\gamma} \\ &\times (p_{N-1} - p_N)^{1/2} H\left(\frac{p_N}{p_{N-1}}-\beta\right) H\left(\frac{p_{N-1}}{p_N}-1\right)\end{aligned} \tag{25}$$

V. Simple One-Dimensional Case

Equations (20–22) for the adiabatic case and Eqs. (23–25) for the isothermal case are easily solved using the fourth-order Runge–Kutta method, giving the initial conditions.

The model is applied to a string of identical cells in the shape of cuboids, connected by identical holes (see Fig. 5). The parameters are $T_0 = 290$ K, $p_0 = 1,013,500$ dyne/cm^2 (1 atm), $V = 1.117$ cm^3, and $a = 0.0001824$ cm^2 for all cells. The gas used is argon.

We are only interested in the case of $N \gg 1$, such that it does not matter much whether N is even or odd. By symmetry, we only have to deal with the half of the string that has $n = N/2$ cells. Let the punctured cells be labeled by i, from one to n, going from the cell at the center to the cell at one end.

A. Adiabatic Case

For the $i = 1$ cell in Fig. 5, the pressure is dictated by the exchange of gas with the next cell $i = 2$ on its right, through their common hole. The same occurs between the $i = 1$ cell and the cell to its left. No critical flow is expected here. Equation (20) for cell 1 is replaced by

$$\begin{aligned}\frac{\mathrm{d}p_1}{\mathrm{d}t} =& -2CH_A \frac{a}{V} p_1^{1-(1/\gamma)} \left(\frac{p_1+p_2}{2}\right)^{1/2\gamma} (p_1-p_2)^{1/2} H\left(\frac{p_1}{p_2}-1\right) \\ &+ 2CH_A \frac{a}{V} p_2^{1-(1/\gamma)} \left(\frac{p_1+p_2}{2}\right)^{1/2\gamma} (p_2-p_1)^{1/2} H\left(\frac{p_2}{p_1}-1\right)\end{aligned} \tag{26}$$

where p_1 and p_2 are the pressures in cells 1 and 2, respectively. Equation (21) is rewritten as, for cells i, from two to $n-1$,

$$\begin{aligned}\frac{\mathrm{d}p_i}{\mathrm{d}t} =& -\Gamma_A \frac{a}{V} K_A p_i^{\lambda} H\left(\beta - \frac{p_{i-1}}{p_i}\right) - \Gamma_A \frac{a}{V} K_A p_i^{\lambda} H\left(\beta - \frac{p_{i+1}}{p_i}\right) \\ &+ \Gamma_A \frac{a}{V} K_A p_{i-1}^{\lambda} H\left(\beta - \frac{p_i}{p_{i-1}}\right) + \Gamma_A \frac{a}{V} K_A p_{i+1}^{\lambda} H\left(\beta - \frac{p_i}{p_{i+1}}\right) \\ &- CH_A \frac{a}{V} p_i^{1-(1/\gamma)} \left(\frac{p_i+p_{i-1}}{2}\right)^{1/2\gamma} (p_i - p_{i-1})^{1/2} \\ &\times H\left(\frac{p_{i-1}}{p_i}-\beta\right) H\left(\frac{p_i}{p_{i-1}}-1\right) - CH_A \frac{a}{V} p_i^{1-(1/\gamma)} \left(\frac{p_i+p_{i+1}}{2}\right)^{1/2\gamma} \\ &\times (p_i - p_{i+1})^{1/2} H\left(\frac{p_{i+1}}{p_i}-\beta\right) H\left(\frac{p_i}{p_{i+1}}-1\right) \\ &+ CH_A \frac{a}{V} p_{i-1}^{1-(1/\gamma)} \left(\frac{p_i+p_{i-1}}{2}\right)^{1/2\gamma} (p_{i-1} - p_i)^{1/2} \\ &\times H\left(\frac{p_i}{p_{i-1}}-\beta\right) H\left(\frac{p_{i-1}}{p_i}-1\right) + CH_A \frac{a}{V} p_{i+1}^{1-(1/\gamma)} \left(\frac{p_i+p_{i+1}}{2}\right)^{1/2\gamma} \\ &\times (p_{i+1} - p_i)^{1/2} H\left(\frac{p_i}{p_{i+1}}-\beta\right) H\left(\frac{p_{i+1}}{p_i}-1\right)\end{aligned} \tag{27}$$

Equation (22) is rewritten as, for cell n,

$$\begin{aligned}\frac{\mathrm{d}p_n}{\mathrm{d}t} =& -\Gamma_I \frac{a}{V} c_0 p_n - \Gamma_I \frac{a}{V} c_0 p_n H\left(\beta - \frac{p_{n-1}}{p_n}\right) \\ &+ \Gamma_I \frac{a}{V} c_0 p_{n-1} H\left(\beta - \frac{p_n}{p_{n-1}}\right) \\ &- C \frac{a}{V} \frac{c_0}{\gamma^{1/2}} p_n^{(1/2)[1-(1/\gamma)]} \left(\frac{p_{n-1}+p_n}{2}\right)^{1/2\gamma} \\ &\times (p_n - p_{n-1})^{1/2} H\left(\frac{p_{n-1}}{p_n}-\beta\right) H\left(\frac{p_n}{p_{n-1}}-1\right) \\ &+ C \frac{a}{V} \frac{c_0}{\gamma^{1/2}} p_{n-1}^{(1/2)[1-(1/\gamma)]} \left(\frac{p_{n-1}+p_n}{2}\right)^{1/2\gamma} \\ &\times (p_{n-1} - p_n)^{1/2} H\left(\frac{p_n}{p_{n-1}}-\beta\right) H\left(\frac{p_{n-1}}{p_n}-1\right)\end{aligned} \tag{28}$$

B. Isothermal Case

For cell 1 in Fig. 5, Eq. (23) becomes

$$\frac{\mathrm{d}p_1}{\mathrm{d}t} = -2C\frac{a}{V}\frac{c_0}{\gamma^{1/2}}p_1^{(1/2)[1-(1/\gamma)]}\left(\frac{p_1+p_2}{2}\right)^{1/2\gamma}(p_1-p_2)^{1/2} \times H\left(\frac{p_1}{p_2}-1\right) + 2C\frac{a}{V}\frac{c_0}{\gamma^{1/2}}p_2^{(1/2)[1-(1/\gamma)]}\left(\frac{p_1+p_2}{2}\right)^{1/2\gamma} \times (p_2-p_1)^{1/2}H\left(\frac{p_2}{p_1}-1\right) \tag{29}$$

For cells i, from two to $n-1$, Eq. (24) becomes

$$\begin{aligned}\frac{\mathrm{d}p_i}{\mathrm{d}t} &= -\Gamma_I\frac{a}{V}c_0p_iH\left(\beta-\frac{p_{i-1}}{p_i}\right) - \Gamma_I\frac{a}{V}c_0p_iH\left(\beta-\frac{p_{i+1}}{p_i}\right) \\ &+ \Gamma_I\frac{a}{V}c_0p_{i-1}H\left(\beta-\frac{p_i}{p_{i-1}}\right) + \Gamma_I\frac{a}{V}c_0p_{i+1}H\left(\beta-\frac{p_i}{p_{i+1}}\right) \\ &- C\frac{a}{V}\frac{c_0}{\gamma^{1/2}}p_i^{(1/2)[1-(1/\gamma)]}\left(\frac{p_{i-1}+p_i}{2}\right)^{1/2\gamma} \\ &\times (p_i-p_{i-1})^{1/2}H\left(\frac{p_{i-1}}{p_i}-\beta\right)H\left(\frac{p_i}{p_{i-1}}-1\right) \\ &- C\frac{a}{V}\frac{c_0}{\gamma^{1/2}}p_i^{(1/2)[1-(1/\gamma)]}\left(\frac{p_i+p_{i+1}}{2}\right)^{1/2\gamma} \\ &(p_i-p_{i+1})^{1/2}H\left(\frac{p_{i+1}}{p_i}-\beta\right)H\left(\frac{p_i}{p_{i+1}}-1\right) \\ &+ C\frac{a}{V}\frac{c_0}{\gamma^{1/2}}p_{i-1}^{(1/2)[1-(1/\gamma)]}\left(\frac{p_{i-1}+p_i}{2}\right)^{1/2\gamma} \\ &(p_{i-1}-p_i)^{1/2}H\left(\frac{p_i}{p_{i-1}}-\beta\right)H\left(\frac{p_{i-1}}{p_i}-1\right) \\ &+ C\frac{a}{V}\frac{c_0}{\gamma^{1/2}}p_{i+1}^{(1/2)[1-(1/\gamma)]}\left(\frac{p_i+p_{i+1}}{2}\right)^{1/2\gamma} \\ &\times (p_{i+1}-p_i)^{1/2}H\left(\frac{p_i}{p_{i+1}}-\beta\right)H\left(\frac{p_{i+1}}{p_i}-1\right)\end{aligned} \tag{30}$$

For the last cell n, Eq. (25) becomes

$$\begin{aligned}\frac{\mathrm{d}p_n}{\mathrm{d}t} &= -\Gamma_I\frac{a}{V}c_0p_n - \Gamma_I\frac{a}{V}c_0p_nH\left(\beta-\frac{p_{n-1}}{p_n}\right) \\ &+ \Gamma_I\frac{a}{V}c_0p_{n-1}H\left(\beta-\frac{p_n}{p_{n-1}}\right) \\ &- C\frac{a}{V}\frac{c_0}{\gamma^{1/2}}p_n^{(1/2)[1-(1/\gamma)]}\left(\frac{p_{n-1}+p_n}{2}\right)^{1/2\gamma} \\ &\times (p_n-p_{n-1})^{1/2}H\left(\frac{p_{n-1}}{p_n}-\beta\right)H\left(\frac{p_n}{p_{n-1}}-1\right) \\ &+ C\frac{a}{V}\frac{c_0}{\gamma^{1/2}}p_{n-1}^{(1/2)[1-(1/\gamma)]}\left(\frac{p_{n-1}+p_n}{2}\right)^{1/2\gamma} \\ &\times (p_{n-1}-p_n)^{1/2}H\left(\frac{p_n}{p_{n-1}}-\beta\right)H\left(\frac{p_{n-1}}{p_n}-1\right)\end{aligned} \tag{31}$$

In both Eqs. (27) and (30), the first four terms come from consideration of choked flow, which is not expected to be important, except for the end cell. Similarly, in both Eqs. (28) and (31), the second and third terms account for any exchange of gas through choked flow between cell n and cell $n-1$, but that exchange is unlikely, as choked flow is expected to be important only between the cell n and the adjacent vacuum.

C. Numerical Results

For each of the adiabatic and isothermal cases, $N = 100, 200, 300,$ and 400 are considered. Let $P = p/p_0$, where $p = p(i) = p_i$. For the adiabatic case, the plots of P (in atmospheres) vs t are shown in Fig. 6. A typical profile of P vs i is shown in Fig. 7. The plots of

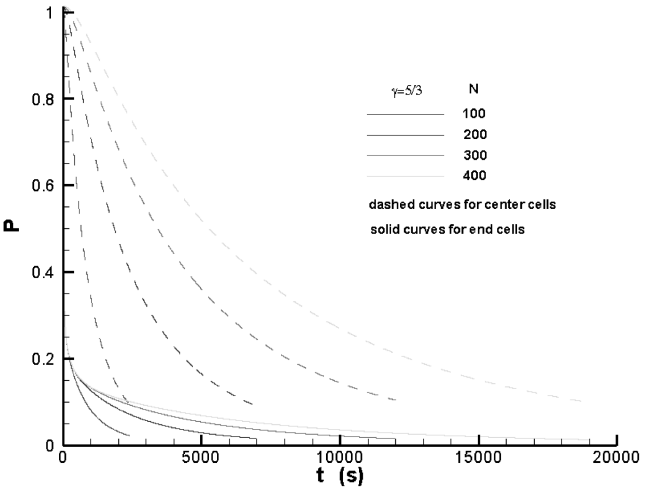

Fig. 6 P vs t for center and end cells for various Ns in the adiabatic case.

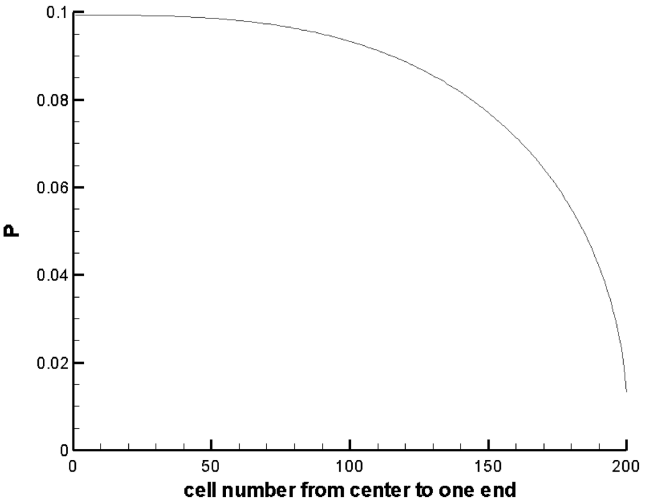

Fig. 7 Profile of P vs x in half-string of cells at $t = 19,000$ s for $N = 400$ in the adiabatic case.

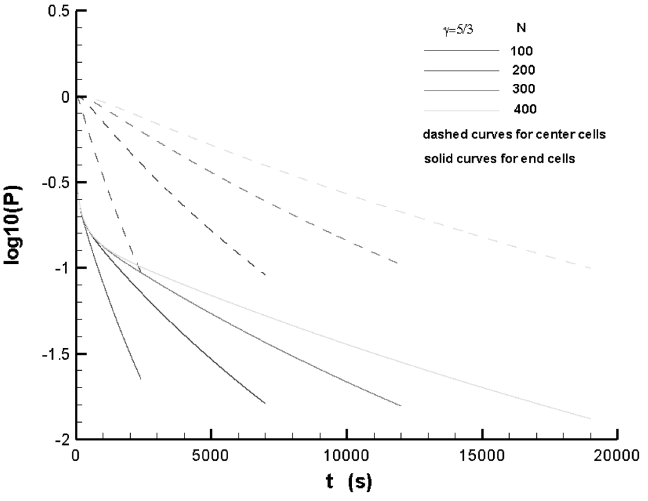

Fig. 8 $\log_{10}(P)$ vs t in center and end cells for various Ns in the adiabatic case.

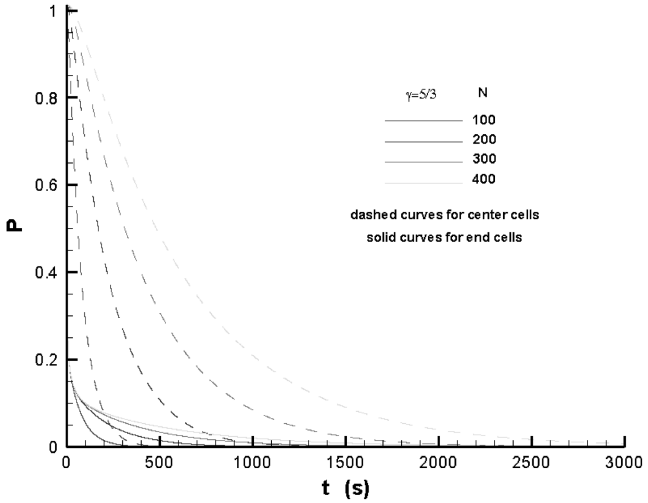

Fig. 9 ***P*** **vs** ***t*** **in center and end cells for various** ***N*****s in the isothermal case.**

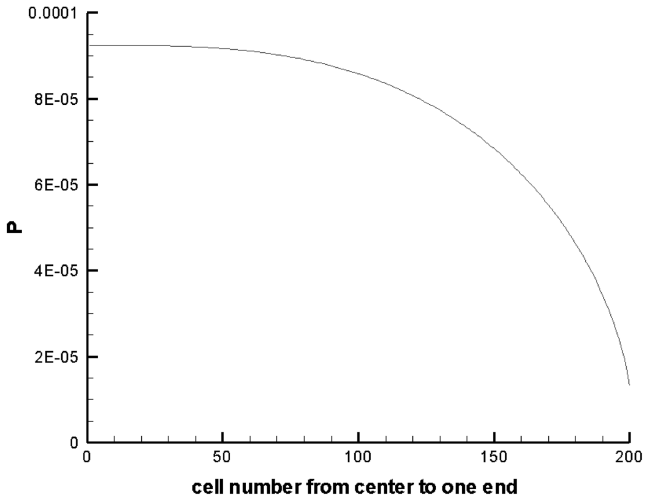

Fig. 10 Profile of ***P*** **vs** ***x*** **in half-string at** $t = 5600$ **s for** $N = 400$ **in the isothermal case.**

$\log_{10}(P)$ vs t are shown in Fig. 8. Similarly, for the isothermal case, the plots of P vs t are shown in Fig. 9. A typical profile of P vs i is shown in Fig. 10. The plots of $\log_{10}(P)$ vs t are shown in Fig. 11. In the more revealing Figs. 8 and 11, for each N, the slope of the curve of the center cell and that of the end cell are similar, if not parallel, with each other, especially with increasing t. Noting that the slopes for different Ns vary widely, these two observations imply the existence of a scaling law.

VI. Scaling Law

The scaling law is found unexpectedly in the attempt to replace the discrete model, represented by Eqs. (26–31), with a continuum model for large N for computational efficiency.

The transition from the discrete model to a continuum model starts with the approximation $p_{i+1} = p_i + \partial p_i \partial i + (1/2)\partial^2 p_i \partial i^2$ and $p_{i-1} = p_i - \partial p_i \partial i + (1/2)\partial^2 p_i \partial i^2$ in the expressions $p_{i\pm1} - p_i$ in the discrete equations. Other than that, $p_{i\pm1}$ is simply replaced by p_i. For large n, i is replaced by $x = i/n$, where $0 < x < 1$, and p_i is replaced by $P(x, t) = p_i/p_0$. Let t be replaced by $T = t/\tau$, where τ is the time scale to be determined. By assuming that the gas only flows toward the end cell and that critical flow is important only for the end cell, many terms in the equations for the discrete model can be simplified and even dropped.

For the adiabatic case, Eq. (27) becomes

$$\frac{\partial P}{\partial T} = -\tau \frac{CH_A}{n}\frac{a}{V} p_0^{(1/2)-(1/2\gamma)} P^{1-(1/2\gamma)} \times \left[\left(-n\frac{\partial P}{\partial x} - \frac{1}{2}\frac{\partial^2 P}{\partial x^2}\right)^{1/2} - \left(-n\frac{\partial P}{\partial x} + \frac{1}{2}\frac{\partial^2 P}{\partial x^2}\right)^{1/2}\right] \tag{32}$$

It is expected that $\partial P/\partial x \le 0$, where $\partial P/\partial x = 0$, $\partial^2 P/\partial x^2 = 0$, and the right side is zero. But where $\partial P/\partial x < 0$, $\partial^2 P/\partial x^2$ is treated as a correction term, such that the two quantities inside the square bracket on the right side can be expanded binomially, giving, after simplification,

$$\frac{\partial P}{\partial T} = (2\gamma)^{1/2} C P^{1-(1/2\gamma)} \frac{\partial^2 P/\partial x^2}{(-\partial P/\partial x)^{1/2}} \tag{33}$$

where we have let

$$\tau = \frac{N^{\frac{3}{2}}}{c_0}\frac{V}{a} \tag{34}$$

Similarly, for the isothermal case, Eq. (30) becomes

$$\frac{\partial P}{\partial T} = -\tau \frac{C}{n}\frac{a}{V}\frac{c_0}{\gamma^{1/2}} P^{1/2} \times \left[\left(-n\frac{\partial P}{\partial x} - \frac{1}{2}\frac{\partial^2 P}{\partial x^2}\right)^{1/2} - \left(-n\frac{\partial P}{\partial x} + \frac{1}{2}\frac{\partial^2 P}{\partial x^2}\right)^{1/2}\right] \tag{35}$$

Again, using binomial expansion, we obtain, after simplification,

$$\frac{\partial P}{\partial T} = \left(\frac{2}{\gamma}\right)^{1/2} C P^{1/2} \frac{\partial^2 P/\partial x^2}{(-\partial P/\partial x)^{1/2}} \tag{36}$$

where τ is also given by Eq. (34). Note that Eqs. (33) and (35) are nonlinear diffusion equations, with $\partial P/\partial T$ on the left and $\partial^2 P/\partial x^2$ on the right, with the positive diffusion coefficient depending on P and $\partial P/\partial x$.

The boundary conditions for the continuum model, for both the adiabatic and isothermal cases, are

$$\left(\frac{\partial P}{\partial x}\right)_{x=0} = 0 \tag{37}$$

and

$$n^2 q(P)_{x=1} = -n\left(\frac{\partial P}{\partial x}\right)_{x=1} - \frac{1}{2}\left(\frac{\partial^2 P}{\partial x^2}\right)_{x=1} \tag{38}$$

where $q = 2(1-\beta)\beta^{1/\gamma}$. Equation (38) is obtained by equating what corresponds to the first term on the right side of Eq. (28) or Eq. (31) with the first term on the right side of Eq. (32) or Eq. (35), respectively. Now the model is completely dimensionless, depending only on γ in the diffusion equations (33) or (36) and the boundary condition in Eq. (38), and n in the boundary condition in Eq. (38).

With the continuum model, instead of dealing with n cells, we can deal with m grid points for the x domain, where $m \ll n$, allowing for a much faster computation, where n is large. For example, with $N = 400$ (i.e., $n = 200$), m can be as small as 25, because P is a smooth function of x (see Figs. 6 and 9).

The continuum model gives results that are qualitatively similar to those of the discrete model. However, it has turned out to be not very accurate for the following reason. For a uniform grid of x, with $m \ll n$, the grid size Δx covers many cells, thus saving much computational effort. However, this advantage is a disadvantage at the end cell. Since this cell is subjected to critical flow on one side and subcritical flow on the other, $\partial P/\partial x$ and $\partial^2 P/\partial x^2$ can change quite rapidly in there. This is beyond the resolution of the continuum model with the relatively large Δx. It follows that the boundary condition at $x = 1$ of the continuum model cannot be accurate enough. It might be possible to refine the numerical procedure or modify the boundary condition at $x = 1$ to improve the performance

of the continuum model. But for the size of N of interest, the computational work with the discrete model is bearable enough. Nevertheless, the derivation of the continuum model reveals that the time scale of the system is τ, as given by Eq. (34).

VII. Dimensionless Results of the Simple One-Dimensional Case

The results can now be presented in dimensionless forms with $P = p/p_0$ and $T = t/\tau$. The values of τ are listed in Table 1 for easy reference.

Figures 8 and 11 can be redrawn as Figs. 12 and 13. With the time scale τ, the scattered curves for the center cells in Figs. 8 and 11 collapse into one curve. Although those for the end cells do not do so, their slopes converge to the same value at large T. This indicates that steady states appear at large T.

A steady state is attained when the pressures at the center and end cells decay in a coordinate manner. The curves for the end cells do not collapse into one curve, because it takes finite time for the leak at the end cell to reach the center cell, and larger N requires longer time.

The isothermal decay is exponential at large T, with the pressure in the center cell going like $P \approx 10^{-1.2T}$. The adiabatic decay at large T is not as clearly exponential, but the slope also seems to approach a constant value of approximately 0.07, such that $P \approx 10^{-0.07T}$. For the pressure in the center cell to drop by a factor of 10^{-5} from the initial value of 1 atm, the time required is thus estimated to be of the order of 30 h for the adiabatic case and of 2 h for the isothermal case. Since we are mostly interested in the faster drain of the gas from the structure, we shall accordingly only consider the isothermal case next.

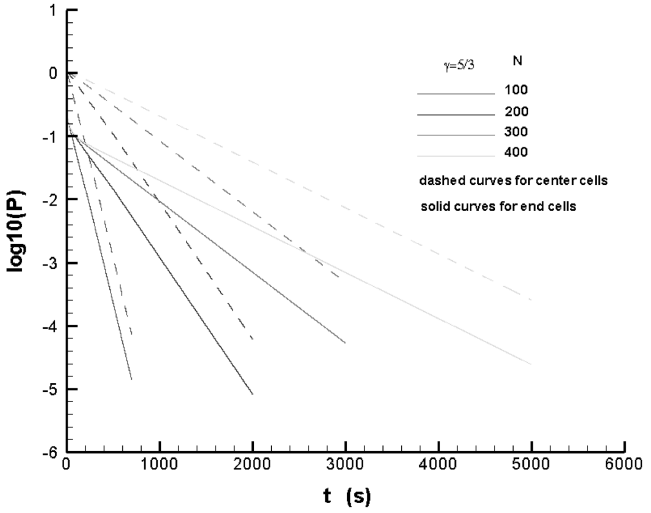

Fig. 11 Log10(P) vs t in center and end cells for various N's in the isothermal case.

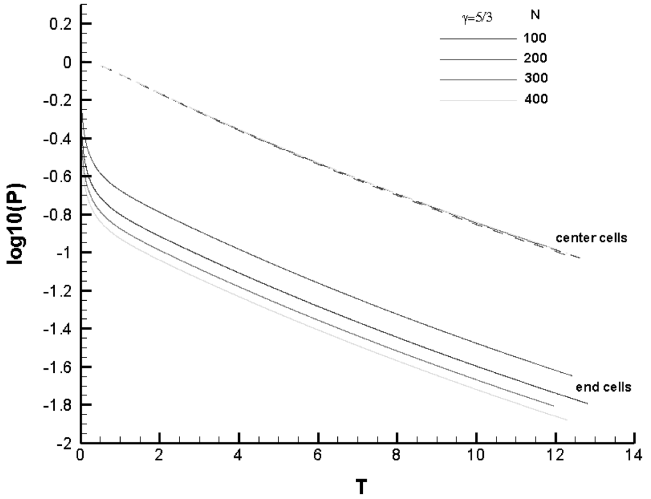

Fig. 12 Dimensionless plot of $\log_{10}(P)$ vs T in center and end cells for various Ns in the adiabatic case.

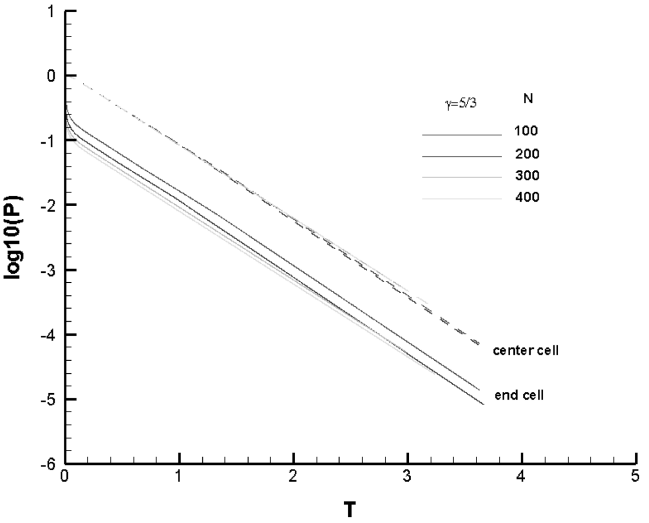

Fig. 13 Dimensionless plot of $\log_{10}(P)$ vs T in center and end cells for various Ns in the isothermal case.

VIII. Two-Dimensional Isothermal Honeycomb Structure

Consider now an isothermal two-dimensional honeycomb structure, such as the one shown in Fig. 14. It consists of cells having hexagonal cross sections, each connected to six other adjacent cells, with the common walls perforated by pinholes. Let the cells be given the same parameters as those in the simple one-dimensional case: $T_0 = 290$ K, $p_0 = 1,013,500$ dyne/cm^2, $V = 1.117$ cm^3, and $a = 0.0001824$ cm^2 for all cells. The gas used is argon.

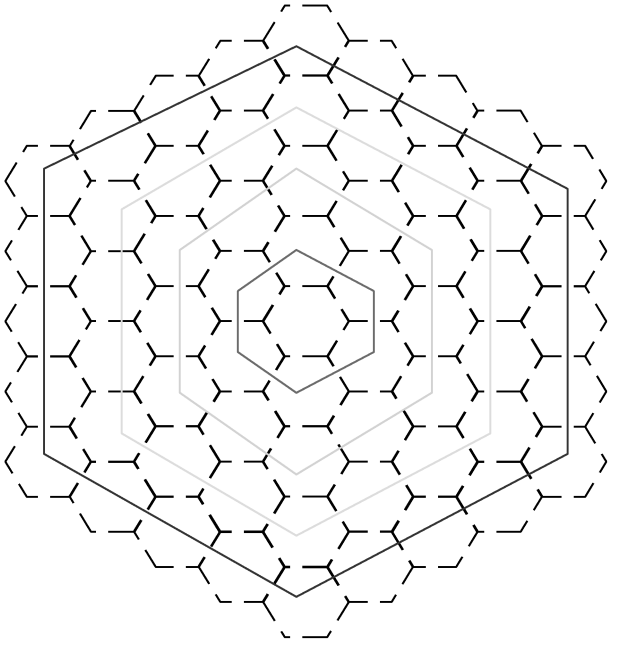

Fig. 14 Honeycomb structure with each hexagon having each of its six walls perforated. The innermost hexagon marks the first layer of cells ($i = 2$) surrounding the core cell ($i = 1$). Similarly, the remaining hexagons (from the inside out) mark the second ($i = 3$), third ($i = 4$), and fourth ($i = 5$) layers, etc.

Table 1 One-dimensional system of cells: characteristic time scale τ vs number of cells N, with τ going like $N^{3/2}$

N	τ, s
100	193
200	546
300	1003
400	1545
500	2159
600	2838
700	3576
800	4369
900	5213
1000	6106
1100	7044
1200	8026
1300	9050
1400	10114

The two-dimensional problem can be simplified into a one-dimensional one as follows. The cell at the center is connected to six cells. If the center cell is called the first (or $i = 1$) layer, then the six cells surrounding it constitute the $i = 2$ layer. The layer of cells next to these six cells is called the $i = 3$ layer, and so on. In each layer, there are pinholes facing outward and pinholes facing inward from the layer. There are also pinholes between adjacent cells in the layer. But there is no gas flow among the cells in a given layer because of k-fold symmetry, where k is the number of cells in that layer. Thus, we can concentrate on the gas flow in the radial direction. For each layer, we are interested in the number of cells, the number of pinholes facing outward, and the number of pinholes facing inward. These numbers are displayed in Table 2.

Let there be n layers in the honeycomb structure. It can be generalized that, for the ith layer, where $i = 2, 3, \ldots$, the number of cells is $6(i-1)$, the number of holes on the inside is $12i - 18$, and the number of holes on the outside is $12i - 6$. If the number of layers is n, then the total number of cells is $M = 3n^2 - 3n + 1$. For large n, $M \approx 3n^2 \approx \pi n^2$, such that n can be considered as the radius of the structure in terms of cells, M its area, and $N = 2n$ its diameter.

As seen in Fig. 15, in each layer for $i > 2$, there are six cells at the corners of the hexagonal layer, each of which has three outward-facing pinholes and one inward-facing pinhole. For the rest, each has two outward-facing pinholes and two inward-facing pinholes. Thus, the pressure inside such a layer is not expected to be exactly uniform, and there can be some gas flow along the layer. But, we shall ignore this and assume axisymmetry for the system about the center cell.

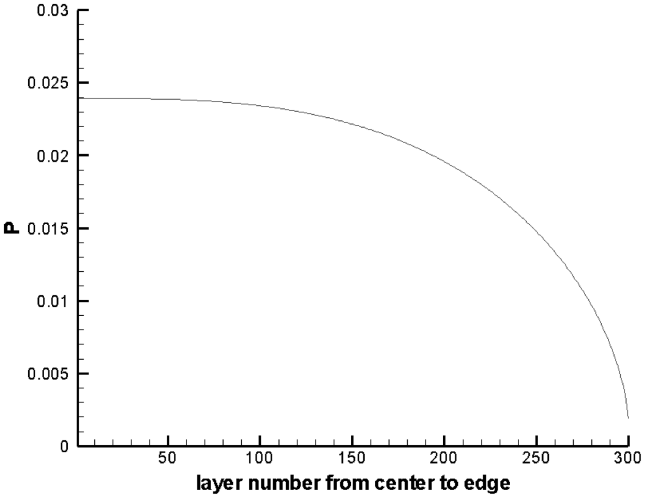

Fig. 15 Profile of P along radius of isothermal hexagonal structure for 269,101 cells at $t = 4200$ s.

Table 2 Two-dimensional hexagonal system of cells: Relation among the cell-layer label and number of cells it contains, the number of holes on the inside of the layer, and the number of holes on its outside

ith layer	No. of cells	No. of holes on inside of layer	No. of holes on outside of layer
1 (core)	1	0	6
2	6	6	18
3	12	18	30
4	18	30	42
5	24	42	54
i	$6(i-1)$	$12i - 18$	$12i - 6$

For $i > 1$, the ith layer of cells can be considered as a single cell i by letting $V_i = 6(i-1)V$, with the area of the single outward-facing pinhole as $a_{i,i+1} = (12i - 6)a$, and that of the single inward-facing pinhole as $a_{i,i-1} = (12i - 18)a$, in Eqs. (23–25). Defining

$$u_i = \frac{2i-3}{i-1} \tag{39a}$$

and

$$v_i = \frac{2i-1}{i-1} \tag{39b}$$

the isothermal one-dimensional equations (29–31) are replaced by

$$\begin{aligned}\frac{\mathrm{d}p_1}{\mathrm{d}t} &= -6C\frac{a}{V}\frac{c_0}{\gamma^{1/2}}p_1^{(1/2)[1-(1/\gamma)]}\left(\frac{p_1+p_2}{2}\right)^{1/2\gamma}(p_1-p_2)^{1/2}\\ &\quad\times H\left(\frac{p_1}{p_2}-1\right)+6C\frac{a}{V}\frac{c_0}{\gamma^{1/2}}p_2^{(1/2)[1-(1/\gamma)]}\left(\frac{p_1+p_2}{2}\right)^{1/2\gamma}\\ &\quad\times(p_2-p_1)^{1/2}H\left(\frac{p_2}{p_1}-1\right)\end{aligned} \tag{40}$$

$$\begin{aligned}\frac{\mathrm{d}p_i}{\mathrm{d}t} &= -\Gamma_I u_i\frac{a}{V}c_0p_iH\left(\beta-\frac{p_{i-1}}{p_i}\right)-\Gamma_I v_i\frac{a}{V}c_0p_iH\left(\beta-\frac{p_{i+1}}{p_i}\right)\\ &\quad+\Gamma_I u_i\frac{a}{V}c_0p_{i-1}H\left(\beta-\frac{p_i}{p_{i-1}}\right)\\ &\quad+\Gamma_I v_i\frac{a}{V}c_0p_{i+1}H\left(\beta-\frac{p_i}{p_{i+1}}\right)\\ &\quad-Cu_i\frac{a}{V}\frac{c_0}{\gamma^{1/2}}p_i^{(1/2)[1-(1/\gamma)]}\left(\frac{p_{i-1}+p_i}{2}\right)^{1/2\gamma}\\ &\quad(p_i-p_{i-1})^{1/2}H\left(\frac{p_{i-1}}{p_i}-\beta\right)H\left(\frac{p_i}{p_{i-1}}-1\right)\\ &\quad-Cv_i\frac{a}{V}\frac{c_0}{\gamma^{1/2}}p_i^{(1/2)[1-(1/\gamma)]}\left(\frac{p_i+p_{i+1}}{2}\right)^{1/2\gamma}\\ &\quad\times(p_i-p_{i+1})^{1/2}H\left(\frac{p_{i+1}}{p_i}-\beta\right)H\left(\frac{p_i}{p_{i+1}}-1\right)\\ &\quad+Cu_i\frac{a}{V}\frac{c_0}{\gamma^{1/2}}p_{i-1}^{(1/2)[1-(1/\gamma)]}\left(\frac{p_{i-1}+p_i}{2}\right)^{1/2\gamma}\\ &\quad\times(p_{i-1}-p_i)^{1/2}H\left(\frac{p_i}{p_{i-1}}-\beta\right)H\left(\frac{p_{i-1}}{p_i}-1\right)\\ &\quad+Cv_i\frac{a}{V}\frac{c_0}{\gamma^{1/2}}p_{i+1}^{(1/2)[1-(1/\gamma)]}\left(\frac{p_i+p_{i+1}}{2}\right)^{1/2\gamma}\\ &\quad\times(p_{i+1}-p_i)^{1/2}H\left(\frac{p_i}{p_{i+1}}-\beta\right)H\left(\frac{p_{i+1}}{p_i}-1\right)\end{aligned} \tag{41}$$

and

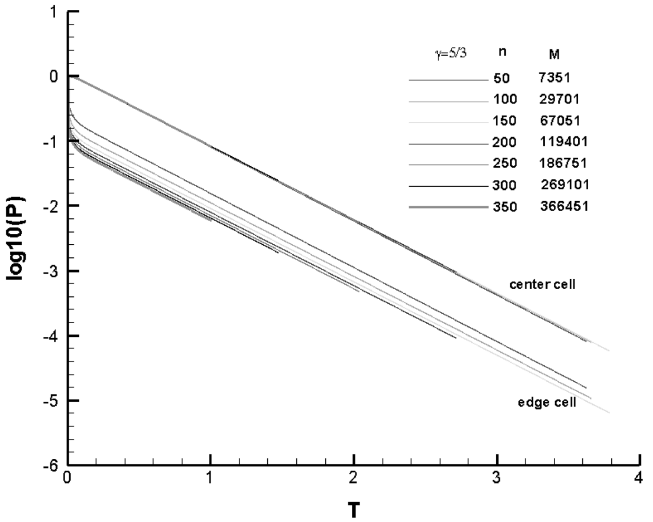

Fig. 16 Dimensionless plot of $\log_{10}(P)$ vs T in center and edge cells for various ns in the isothermal hexagonal structure.

$$
\begin{aligned}
\frac{\mathrm{d}p_n}{\mathrm{d}t} &= -\Gamma_I v_n \frac{a}{V} c_0 p_n - \Gamma_I u_n \frac{a}{V} c_0 p_n H\left(\beta - \frac{p_{n-1}}{p_n}\right) \\
&\quad + \Gamma_I u_n \frac{a}{V} c_0 p_{n-1} H\left(\beta - \frac{p_n}{p_{n-1}}\right) \\
&\quad - C u_n \frac{a}{V} \frac{c_0}{\gamma^{1/2}} p_n^{(1/2)[1-(1/\gamma)]} \left(\frac{p_{n-1}+p_n}{2}\right)^{1/2\gamma} \\
&\quad \times (p_n - p_{n-1})^{1/2} H\left(\frac{p_{n-1}}{p_n} - \beta\right) H\left(\frac{p_n}{p_{n-1}} - 1\right) \\
&\quad + C u_n \frac{a}{V} \frac{c_0}{\gamma^{1/2}} p_{n-1}^{(1/2)[1-(1/\gamma)]} \left(\frac{p_{n-1}+p_n}{2}\right)^{1/2\gamma} \\
&\quad \times (p_{n-1} - p_n)^{1/2} H\left(\frac{p_n}{p_{n-1}} - \beta\right) H\left(\frac{p_{n-1}}{p_n} - 1\right) \qquad (42)
\end{aligned}
$$

In Eq. (40), the factor six comes from the hexagonal geometry.

The numerical results are similar to those of the one-dimensional case. In Fig. 15, a typical profile of $P = p/p_0$ along the radius of the hexagonal structure, of $n = 300$ layers or $M = 269,101$ cells at $t = 4200$ s, is plotted. In Fig. 16, the dimensionless counterpart of Fig. 14 is plotted by scaling t with τ from Eq. (34), showing the same scaling law. The slope is about 1.1, such that P in the center cell is approximately given by $P \approx 10^{-1.1T}$. Hence, for a very large structure of, say $M \approx 1,500,000$ cells, corresponding to $N \approx 1400$ and $\tau = 10,114$ s, the drain time required to reduce the pressure of the center cell from 1 to 10^{-5} atm is estimated to be about 13 h. This, considering the difficulty in modeling such a system, might be assumed as a best-case (minimum time) scenario. Adiabatic conditions, lower temperatures expected during cryopumping, nonuniformities or debris in the perforations, a less direct gas exit path associated with a dome (curved) surface, consequence of pressure gradients within a ring, outgassing of previously adsorbed atoms or molecules, and a higher external environment pressure will all increase the evacuation time.

IX. Conclusions

A model has been developed that predicts the time to drain gas, initially at 1 atm, from a linear series of cells that share a pinhole through their common walls to an outside vacuum environment. As expected, the time for the center cell pressure to drop to a given level was significantly more than that of an outer cell; both times increased with an increasing cell number. Both adiabatic and isothermal cases were examined. The drain time for the adiabatic case was found to be much longer; when the gas expands during the draining scenario, it cools down and loses pressure, thus decreasing the driving force that pushes the gas toward (and out of) the end cell. The linear cases were then extended to a two-dimensional hexagonal, honeycomb network, as might be expected to be implemented in a common bulkhead. Observation and subsequent evaluation of the calculations showed that the pressure results could be scaled in terms of a characteristic time and the number of cells.

The intent was to solve a realistic problem involving more than one million cells. It is expected that a commercial computational fluid dynamics program, if one exists, would require a billion grid points; adapting a program would introduce further problems. Furthermore, it would take days for the computation, even with parallel processing by a network of PCs; the program would also have to be repeatedly run to obtain data, so that the trend could be established. In contrast, the model presented here requires only one PC and a few hours.

Acknowledgments

The authors wish to acknowledge the support of the Marshall Space Flight Center Project Office and EM30. Appreciation is also expressed to Mike McKeown of the Kurt J. Lesker Company for his interest and critical reading of the manuscript.

Reference

[1] Landau, L. D., and Lifshitz, E. M., *Fluid Mechanics*, Pergamon Press, New York, 1979.

G. Agnes
Associate Editor